polymers

MDPI

Article

Anti-inflammatory and osteogenic effect of phloroglucinol-enriched whey protein isolate fibrillar coating on Ti-6Al-4V alloy

Anna Mieszkowska [1,*], Laurine Martocq [2], Andrey Koptyug [3], Maria A Surmeneva [4], Roman A Surmenev [4], Javad Naderi [5], Maria Muchova [6,7], Katarzyna A Gurzawska-Comis [8,9,10], Timothy E L Douglas [2]

[1] Department of Evolutionary Immunology, Institute of Zoology and Biomedical Research, Faculty of Biology, Jagiellonian University, Krakow, Poland; anna.mieszkowska@uj.edu.pl
[2] School of Engineering, Lancaster University, Lancaster LA1 4YW, United Kingdom; laurine.martocq@gmail.com (L.M.); t.douglas@lancaster.ac.uk (T.E.L.D.)
[3] Department of Quality Technology, Mechanical Engineering & Mathematics, Mid Sweden University, 851 70 Östersund, Sweden; andrey.koptyug@miun.se
[4] Physical Materials Science and Composite Materials Centre, Research School of Chemistry & Applied Biomedical Sciences, National Research Tomsk Polytechnic University, 634050 Tomsk, Russia; surmenevamaria@mail.ru (M.A.S.); rsurmenev@mail.ru (R.A.S.)
[5] Chemistry Department, Lancaster University, Lancaster LA1 4YW, United Kingdom; javadnaderi107@gmail.com
[6] Institute for Medical Microbiology and Virology, Leipzig University, Leipzig, Germany; maria.muchova@medizin.uni-leipzig.de
[7] Periodontal Research Group, Birmingham School of Dentistry, Institute of Clinical Sciences, The University of Birmingham, Birmingham, United Kingdom;
[8] Department of Oral Surgery, Liverpool University Dental Hospital, Institute of Life Course and Medical Science, University of Liverpool, Liverpool L3 5PS, United Kingdom; k.gurzawska-comis@liverpool.ac.uk (K.A.G.C.)
[9] Liverpool Head and Neck Centre, University of Liverpool, Liverpool L69 3BX, United Kingdom;
[10] Department of Dentistry and Oral Health, Section for Maxillofacial Surgery and Oral Pathology, Aarhus University, Vennelyst Boulevard 9, Aarhus C DK-8000, Denmark.
* Correspondence: anna.mieszkowska@uj.edu.pl

Abstract: Biomaterials play a crucial role in the long-term success of bone implants treatment. Accumulation of bacterial biofilm on the implants induces inflammation leading to implant failure. Modification of implant surface with bioactive molecules is one of the strategies to improve biomaterial compatibility and limit inflammation. In this study, whey protein isolate (WPI) fibrillar coatings were used as a matrix to incorporate biologically active phenolic compound phloroglucinol (PG) at different concentration (0.1% and 0.5%) on titanium alloy (Ti6Al4V) scaffolds. Successful Ti6Al4V coating was validated by X-ray photoelectron spectroscopy (XPS), showing decrease in %Ti and increases in %C, %N, %O which demonstrate the presence of the protein layer. The biological activity of PG-enriched WPI (WPI/PG) coatings was assessed using bone-forming cells, human bone marrow-derived mesenchymal stem cells (BM-MSCs). WPI/PG coatings modulated behaviour of BM-MSCs, but did not have negative impact on cell viability. WPI with higher concentration of PG increased gene expression relative to osteogenesis and reduced pro-inflammatory response of BM-MSCs after biofilm stimulation. Autoclaving reduced WPI/PG bioactivity compared to filtration. By using WPI/PG coatings, this study addresses the challenge of improving osteogenic potential while limiting biofilm-induced inflammation at the Ti6Al4V surface. These coatings represent a promising strategy to enhance implant bioactivity.

Keywords: Ti6Al4V; fibrillar coating; phenolic coating; whey protein isolate; inflammation; biofilm; osseointegration; osteogenesis; stem cells;

Academic Editor: Firstname Lastname

Received: date
Revised: date
Accepted: date
Published: date

Citation: To be added by editorial staff during production.

1. Introduction

Titanium (Ti) and its alloys, in particular Ti6Al4V, are widely used as primary biomaterials for orthopedic and dental implants due to their good physical-chemical properties and high biocompatibility with host tissues. However, despite these advantages, the implantation of Ti into bone disrupts host tissues and induces an inflammatory response. Immune cells and mesenchymal stem cells (MSCs) that are recruited to the site of implantation play the key role in the bone healing process. MSCs differentiate into mature bone-forming cells and deposit a collagen matrix, leading to bone formation at the implant surface [1,2]. This complex and long-term process could be affected by different factors, including bacterial infections. Shortly after implantation, the surface of Ti implants becomes exposed to bacterial adhesion and biofilm formation. Due to the rich and highly diverse oral microflora, the composition of bacterial biofilm around dental implants is more complex than that on orthopedic implants. *Streptococcus* species play the pivotal role in early colonization of dental implants, while in the later phases of biofilm formation the growth of different periodontal pathogens such *as Fusobacterium nucleatum*, *Prevotella intermedia, Porphyromonas gingivalis* and *Aggregatibacter actinomycetemcomitan*s has been frequently observed [3,4]. Treatment of biofilm-related infections at implant sites is challenging due to the multispecies composition of microbial biofilm. Moreover, the excessive growth of periodontal pathogens induces a local inflammatory response, often progressing to peri-implantitis and ultimately leading to implant failure [5].With the increasing prevalence of antibiotic-resistant bacteria, there is interest in antibacterial strategies which do not rely on antibiotics. These include photoactivation modification of topography, and the use of naturally occurring biomolecules like polyphenols [6–8].

To address bacterial adhesion on Ti surfaces and reduce inflammation, numerous strategies have been developed, primarily focusing on surface modifications with antimicrobial and/or anti-inflammatory coatings [9].

Whey protein isolate (WPI)-based coatings are promising candidates for surface modification of Ti implants [10]. One of the main advantages of using WPI in Ti surface modification is its low production cost, as WPI is a by-product of the dairy industry. In addition, WPI spontaneously form fibrillar structures under acid conditions and high temperature, increasing the surface/volume ratio of the coatings and enhancing cell adhesion and spreading [11,12]. Different studies have demonstrated that WPI fibrils have the ability to increase osteogenic differentiation and exhibit antibacterial properties [13,14]. Furthermore, WPI fibrils can be used as matrices for the incorporation of biologically active molecules such as glycosaminoglycans - components of extracellular matrix (ECM) [15,16]. WPI fibrils have also been successfully modified with biologically active marine-derived polysaccharides, proteins and polyphenols to enhance their osteogenic properties [17]. Numerous studies have confirmed the osteogenic and anti-inflammatory properties of phloroglucinol (PG), a subunit of marine-derived polyphenols [18,19]. PG has been shown to possess the ability to reduce high levels of oxidative stress, which may be one of the most critical factors contributing to bone resorption [20,21]. The antioxidant, antibacterial and osteogenic properties of PG were also described by Lišková et al [22]. More recently, our previous in *vitro* study confirmed that incorporation of PG into collagen fibrils promotes osteogenesis and reduces inflammation. PG-enriched collagen fibrillar coatings on Ti surfaces up-regulated the gene expression of osteogenic markers and down-regulated the gene expression of markers involved in pro-inflammatory response in osteoblast-like cells (SaOS-2) [23]. However, despite their numerous advantages, collagen fibrils cannot withstand sterilization by autoclaving which is a method widely used in biomedical field.

Two significant advantages of WPI fibrils over collagen fibrils are their much lower cost and ability to withstand sterilization by autoclaving, a clinically accepted and cheap, ubiquitous method. A further ethical advantage is that the use of WPI, being derived from

milk, does not involve the slaughter of animals. Therefore, in the following study WPI fibrils were used as matrices for incorporation of PG, which is known for its antibacterial, antioxidant and anti-inflammatory properties, as well as positive impacts on cell adhesion and differentiation [23,24]. To the best of our knowledge, phenolics such as PG have not yet been incorporated into WPI fibril coatings for biomaterial applications. In this context, this work aimed (i) to develop WPI-based fibrillar coatings enriched with PG on Ti6Al4V (Ti) surfaces and (ii) to evaluate the osteogenic and anti-inflammatory properties of these coatings *in vitro*. The atomic composition of the obtained materials was characterized using X-ray photoelectron spectroscopy (XPS). Human bone marrow-derived mesenchymal stem cells (BM-MSCs) were used to assess the osteogenic differentiation potential of PG-enriched WPI coatings, while the anti-inflammatory activity of the coatings was evaluated in response to a multispecies biofilm challenge. Ti6Al4V samples were produced using electron beam melting (EBM®) technology, a 3D printing method where the components are manufactured layer by layer in a vacuum using a metallic precursor powder melted by an intense electron beam, as used in previous work [25]. The use of a 3D printing method to fabricate samples paves the way for the application of this technique with more complicated geometries and internal architectures, which are possible via 3D printing techniques [26].

This study introduces several novel aspects, both biological and material-related. The biological novelty lies in the use of BM-MSCs stimulated with multispecies biofilm, an approach that remains relatively underexplored in the context of biomaterial evaluation. On the material side, this is the first study to use WPI fibrils enriched with PG as a biofunctional coating. Moreover, WPI fibrils are shown to provide a suitable matrix for examining BM-MSC behavior under biofilm challenge. In contrast to our previous work with collagen-based coatings containing PG, this model incorporates biofilm stimulation, enabling a more physiologically relevant assessment in the context of peri-implantitis. WPI coatings also offer great potential for immobilizing bioactive molecules [27], supporting further studies on biofilm–cell–material interactions.

The current study aims to develop natural, cost-effective and bioactive Ti coatings for biomaterial applications to improve bone healing and reduce the risk of implant loss due to biofilm-related infections.

2. Materials and Methods

2.1. Preparation of WPI fibrillar suspensions

WPI was provided by BiPro, Davisco Foods International Inc. (Eden Prairie, MN, USA). WPI fibril suspensions were prepared as previously described by Keppler et al. [28]. A stock solution of WPI in water was prepared at a concentration of 2.5% w/v with stirring until complete dissolution. The pH was adjusted to 2.0 by adding a 2 M HCl solution dropwise. A total of 40 mL of WPI solution was heated in a 100 mL Duran glass bottle at 90°C for 5 hours with a stirring speed of 350 rpm to induce fibril formation, resulting in a fibrillar suspension. The WPI fibrillar suspension was then cooled to 4°C in a water bath to stop the reaction and subsequently stored at 4°C.

PG (Sigma-Aldrich, Gillingham, UK) was incorporated into the WPI fibrillar suspensions as illustrated in Figure 1.

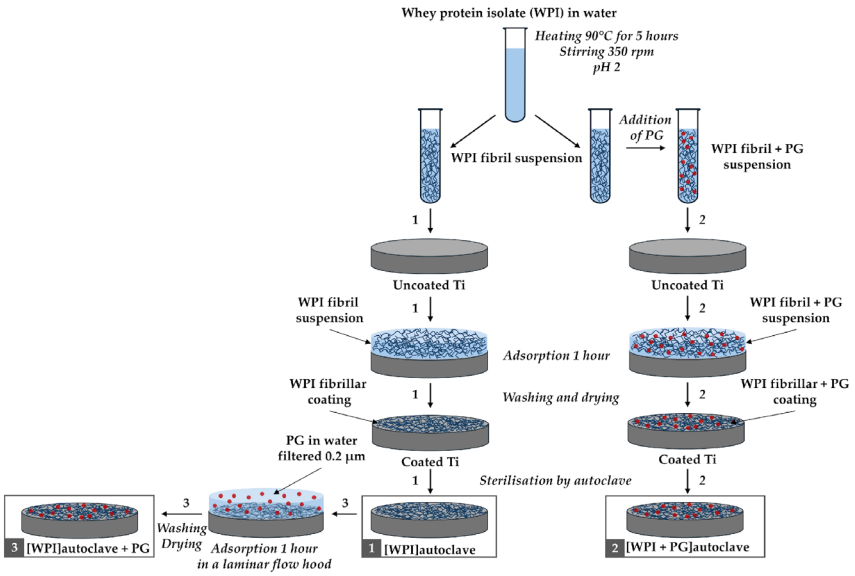

Figure 1. Diagram of the WPI coating process with PG. Three different coating methods are illustrated: (1) WPI coating only, (2) WPI + PG coating autoclaved together, and (3) WPI + PG coating with PG added after the sterilization of the WPI coating. Ti: titanium alloy Ti6Al4V; WPI: whey protein isolate; PG: phloroglucinol.

After cooling the WPI fibrillar suspension in cold water (4°C), PG was added to obtain suspensions enriched with PG at two different concentrations: 0.1%, and 0.5% w/v. Another method for preparing WPI fibril coatings enriched with PG involved the adsorption of PG onto the surface of WPI fibrillar coatings, as described in section 2.2 and illustrated in Figure 1.

2.2. Preparation and characterization of WPI fibrillar coatings

Ti6Al4V (Ti) discs (10 mm diameter and 2 mm thick) were produced using electron beam melting (EBM®) technology, where the components are manufactured layer by layer in a vacuum using a metallic precursor powder melted by an intense electron beam, as previously described [23,29].

The Ti discs were first cleaned with ethanol and water. A WPI fibril suspension was then applied to the Ti6Al4V discs and left for 1 hour to allow fibril adsorption, as shown in Figure 1. After rinsing three times with ultrapure Milli-Q water (Milli-Q, Merck Millipore, Burlington, MA, USA) to remove non-adhered fibrils and drying at room temperature, the Ti discs were coated with a thin layer of WPI fibrils. Finally, these coatings were sterilized by autoclaving at 121°C, 1 atm, for 15 minutes. This procedure is represented as Process 1 in Figure 1. The same procedure was followed to create WPI coatings enriched with PG, as described in Processes 2 and 3 in Figure 1. For Process 2, WPI fibrillar suspensions containing PG were used to coat the Ti discs followed the same steps as described earlier. For Process 3, a PG solution in Milli-Q water (0.2 µm filtered) was added on top of an autoclaved WPI fibrillar coating under sterile conditions. PG adsorption was allowed for 1 hour, and the coatings were then washed three times with Milli-Q water and dried at room temperature. Two different concentrations of PG were tested, 0.1% and 0.5% (w/v) in Milli-Q water. The resulting WPI/PG coatings are named as indicated in Table 1.

Table **1.** WPI coatings denomination with and without PG**.**

Coating denomination	Description
[WPI]autoclave	WPI fibrillar coating autoclaved
[WPI + PG 0.1%]autoclave	WPI + PG 0.1% mixed coating autoclaved
[WPI + PG 0.5%]autoclave	WPI + PG 0.5% mixed coating autoclaved
[WPI]autoclave + PG 0.1%	WPI fibrillar coating autoclaved + PG 0.1% added after
[WPI]autoclave + PG 0.5%	WPI fibrillar coating autoclaved + PG 0.5% added after

The XPS was conducted to analyze the surface chemical composition of all samples, including uncoated and WPI/PG-coated Ti discs. The analysis was performed using a Axis Supra spectrometer (Kratos Analytical Ltd., Manchester, UK) equipped with a monochromatic Al Kα source (1.487 keV). Briefly, samples were mounted on a sample holder using carbon tape and an internal flood gun was used for neutralizing charging effects. Wide-scan spectra were acquired with a pass energy of 160 eV and a step size of 1 eV. Measurements were taken at an emission angle of 0° (relative to the surface normal), with the spectrometer operating at a power of 225 W (15 kV × 15 mA) and analyzing an analysis area of 700 × 300 μm. Three separate locations were analyzed for each sample. The acquired spectra were processed using CasaXPS software (version 2.3.22, Casa Software Ltd., Devon, UK). Binding energies were calibrated against C-C component of the C1s peak at 284.8 eV to compensate for surface charging effects. Curve-fitting procedure of the components was performed using Gaussian-Lorentzian function with a linear background. The Kratos experimental sensitivity factors were used in the atomic composition calculations.

WPI fibril coatings were visualized on glass substrates by Scanning Electron Microscopy (SEM) as described previously [24,30]. The same coating process was used as above. Samples were compared before and after autoclaving.

2.3. Bacterial strains and culture conditions

The bacterial strains used in this study were obtained from the Periodontal Research Group culture collection at the Department of Dentistry, University of Birmingham, UK. *Streptococcus mitis* ATCC 49456 and *Aggregatibacter actinomycetemcomitans* ATCC 43718 were cultured for 24 hours at 37°C in a 5% CO_2 atmosphere on horse blood agar plates (Oxoid, Basingstoke, UK). *Fusobacterium nucleatum* ssp. *polymorphum* ATCC 10593 was grown at 37°C in an anaerobic chamber (80% N_2, 10% CO_2, and 10% H_2; Don Whitley DG250 Anaerobic Workstation, Don Whitley Scientific, Bingley, UK) on Schaedler Anaerobe agar plates (Sigma-Aldrich/Merck, Darmstadt, Germany) for 48 hours. *Porphyromonas gingivalis* ATCC 33277 was cultured anaerobically on horse blood agar plates at 37°C for at least 96 hours.

Liquid cultures of *S. mitis* and *A. actinomycetemcomitans* were grown in Brain Heart Infusion broth (Oxoid, Basingstoke, UK), while *F. nucleatum* and *P. gingivalis* were cultured in Schaedler Anaerobe broth (Oxoid, Basingstoke, UK).

2.4. Bacterial biofilm development

Multispecies biofilms were prepared as previously described [31]. Briefly, overnight bacterial cultures were standardized to 1×10^7 colony-forming units/mL in artificial saliva (AS), which was prepared as follows: 0.25% w/v porcine stomach mucins, 0.02% w/v potassium chloride, 0.02% w/v calcium chloride dihydrate, 0.2% w/v yeast extract, 0.5% w/v proteose peptone (all from Sigma-Aldrich/Merck, Darmstadt, Germany), 0.35% w/v

sodium chloride (Thermo Fisher Scientific, Loughborough, UK), and 0.1% w/v Lab-Lemco powder (Oxoid, Basingstoke, UK) in Milli-Q water. Urea was added after autoclaving to a final concentration of 0.05% v/v (Sigma-Aldrich, Gillingham, UK).

To initiate biofilm formation, the standardized *S. mitis* culture was added to a 24-well plate containing 13-mm Thermanox™ coverslips (Thermo Fisher Scientific, Loughborough, UK) and incubated at 37°C with 5% CO_2. After 24 hours, the biofilm supernatant was removed, and the standardized *F. nucleatum* culture was added. The biofilms were then further incubated under anaerobic conditions at 37°C for another 24 hours. The supernatant was removed, and *A. actinomycetemcomitans* and *P. gingivalis* were added. The biofilms were incubated anaerobically for an additional 4 days at 37°C, with AS replaced every 24 hours.

2.5. Analysis of bacterial biofilm structure and composition

The structure of bacterial biofilm was analyzed using scanning electron microscopy (SEM). For SEM imaging, biofilm samples were prepared as previously described [32]. Initially, the biofilms were fixed using 2.5% glutaraldehyde (Agar Scientific, Stansted, UK) in 0.1 M sodium cacodylate buffer (pH 7.4, BioWorld, Dublin, Ireland) for 10 minutes at room temperature. Subsequently, the biofilms were dehydrated through increasing concentrations of ethanol (20%–100%). Next, the biofilms were treated with hexamethyldisilazane (HMDS; Sigma-Aldrich/Merck, Darmstadt, Germany) as a drying agent. After overnight evaporation of the HMDS, the biofilm samples were mounted onto aluminum specimen stubs (Agar Scientific, Stansted, UK), sputter-coated with gold, and visualized using a scanning electron microscope (Zeiss EVO MA10; Zeiss, Göttingen, Germany).

The composition of bacterial biofilm was analyzed using real-time quantitative PCR (qPCR). Briefly, the bacterial biofilm was scraped from the coverslip surface using standard cell scrapers (Thermo Fisher Scientific, Loughborough, UK) and resuspended in 180 µL of digestion buffer (Invitrogen, Carlsbad, CA, USA). Total bacterial DNA was then isolated using the PureLink Genomic DNA kit (Invitrogen, Carlsbad, CA, USA) following manufacturer's instructions. The quality and quantity of the extracted DNA were assessed using NanoDrop spectrophotometer (Thermo Fisher Scientific, Loughborough, UK). Extracted DNA was amplified using primers targeting the 16S ribosomal RNA (rRNA) gene specific to each bacterial species. The primers used were the same as those described previously [33]. Primers sequences are presented in Table 2.

Table 2. Primers targeting 16S rRNA used in qPCR analyses.

Bacteria species	Primer sequence (5′ to 3′) Forward	Primer sequence (5′ to 3′) Reverse
S. mitis	GATACATAGCCGACCTGAG	CCATTGCCGAAGATTCC
P. gingivalis	AGGCAGCTTGCCATACTGCG	ACTGTTAGCAACTACCGATGT
A. actinomycetemcomitans	GAACCTTACCTACTCTTGA-CATCCGAA	TGCAGCACCTGTCT-CAAAGC
F. nucleatum	GGATTTATTGGGCGTAAAGC	GGCATTCCTACAAATATCTACGAA

Briefly, 2.5 µL of total DNA (100 ng) was added to a reaction mix containing 7.5 µL of GoTaq qPCR Master Mix (Promega, Madison, WI, USA), 0.5 µL (10 µM) of each primer (GenoMed, Warsaw, Poland), and 4 µL of H_2O (Promega, Madison, WI, USA). PCR amplification was conducted under the following conditions: 95°C for 10 minutes, followed by 40 cycles of 95°C for 15 seconds, 56°C for 45 seconds, and 72°C for 30 seconds, with a final extension at 72°C for 5 minutes. The number of each bacteria was determined

using a standard curve prepared from serial dilutions of DNA isolated from fresh cultures of each bacterial species.

2.6. BM-MSCs culture and seeding

The study was performed using commercially available human bone marrow-derived mesenchymal stem cells (BM-MSCs; catalog no. PCS-500-012) obtained from the American Type Culture Collection (ATCC; Manassas, VA, USA). The cells were cultured in α-minimum essential medium (α-MEM) (Lonza, Verviers, Belgium) supplemented with 10% fetal bovine serum (FBS) (Invitrogen, Paisley, UK), 100 U/mL penicillin (Sigma-Aldrich, Gillingham, UK), 100 µg/mL streptomycin (Sigma-Aldrich, Gillingham, UK) and incubated at 37 °C in a humidified atmosphere of 95% air and 5% CO_2 until confluence was reached. BM-MSCs at passages 3–5 were used in the present study. For all *in vitro* assays, BM-MSCs were seeded directly onto uncoated Ti discs, Ti discs coated with WPI alone ([WPI] autoclave), or Ti discs coated with WPI enriched with PG at various concentrations ([WPI+PG 0.1%] autoclave, [WPI+PG 0.5%] autoclave, [WPI] autoclave +PG 0.1%, [WPI] autoclave +PG 0.5%), as described earlier in subsection 2.2 and summarized in Table 1. The discs were placed in wells of 48-well tissue culture polystyrene (TCPS) plates (Life technologies, Paisley, UK) at a density of 3×10^4 cells per disc and cultured for 72 hours.

2.7. BM-MSCs: bacterial biofilm challenge

After 72 hours of BM-MSCs cultivation in standard medium, each Ti disc with BM-MSCs was carefully removed from the wells of 48-well TCPS plate using sterile forceps and transferred to the wells of a 24- well TCPS plate (Life technologies, Paisley, UK). BM-MSCs on the Ti discs were washed twice with fresh medium and then subsequently incubated for 2 hours in antibiotic-free medium at 37°C in a 5% CO_2 atmosphere, with one biofilm-coated glass coverslip per well. The glass coverslips were positioned on the ring supports with the biofilm-facing side oriented toward the titanium surface, according to the co-culture set-up as previously described [34]. The distance between BM-MSCs layer and the biofilm-coated coverslip was maintained to allow fluid flow. After 2 hours, the biofilm-coated glass coverslips were removed from all wells, and the Ti discs with BM-MSCs were washed twice with fresh medium. The Ti discs were then cultured for 48 hours in standard medium with antibiotics for further *in vitro* assays, including metabolic activity measurement, morphology assessment and gene expression analysis.

For this study, two experimental groups were established: (i) the unstimulated control group, consisting of BM-MSCs cultured on Ti with and without WPI/PG coatings under standard conditions, without exposure to the biofilm, and (ii) the biofilm-stimulated group, in which BM-MSCs were exposed to biofilm for 2 hours under co-culture conditions as described above.

2.8. SEM evaluation of BM-MSCs on Ti6Al4V alloy

SEM analyzes were conducted to examine attachment, spreading and morphology of BM-MSCS cultured on the surface of tested Ti discs. Briefly, after 72 hours of cell cultivation, the samples were washed three times with phosphate-buffered saline (PBS) for 10 minutes to remove non-adherent cells. The cells were then fixed with 2% glutaraldehyde in 0.1M sodium cacodylate buffer (pH 7.4) for 2 hours at room temperature. Following the removal of the glutaraldehyde solution, the samples were sequentially dehydrated in increasing concentrations of ethanol. Finally, hexamethyldisilane (HMDS; Sigma-Aldrich, Gillingham, UK) was added to each sample and allowed to dry overnight at room temperature. Imaging was performed using a scanning electron microscope (Zeiss, Göttingen, Germany).

2.9. BM-MSCs metabolic activity

The metabolic activity of BM-MSCs was determined 48 hours after biofilm stimulation. Metabolic activity was assessed in both unstimulated and biofilm-stimulated

BM-MSCs in parallel. Briefly, the cell culture medium was replaced with fresh medium containing methylthiazolyldiphenyl-tetrazolium bromide (MTT) (Sigma-Aldrich, Gillingham, UK) at a final concentration of 0,5mg/ml. After 3 hours of incubation at 37°C in a humidified CO_2 incubator, the medium containing MTT was removed and isopropanol with 0.04 N HCl was added to dissolve formazan crystals. The absorbance was measured at 570 nm. All experiments were performed four times in duplicate (n=8).

2.10. BM-MSCs gene expression analysis

To determine gene expression, total RNA was isolated after 48 hours from both unstimulated and biofilm-stimulated BM-MSCs using TRI reagent (Sigma-Aldrich, Gillingham, UK) and the RNeasy Mini Kit (Qiagen, Crawley, UK), following the manufacturer's protocol. The purity and quantity of RNA were measured using NanoDrop spectrophotometer (Thermo Fisher Scientific, Loughborough, UK). The RNA was reverse-transcribed to cDNA using a one-step high-capacity cDNA Reverse Transcription (RT) kit (Applied Biosystems, Warrington, UK) according to the manufacturer's instructions. The qPCR was conducted on a CFX96 Touch Real-Time PCR Detection System (BioRad, Feldkirchen, Germany) using Roche SYBR Green PCR Master Mix (Roche Diagnostics GmbH, Mannheim, Germany). PCR reactions were performed in 10 μL volumes in a 96-well plate (Roche Diagnostics GmbH, Mannheim, Germany), with each reaction containing 1 μL of cDNA and 9 μL of the reaction mixture, as per the manufacturer's specifications. All samples were amplified in duplicates. The PCR conditions included an initial denaturation step at 95°C for 5 minutes, followed by 40 cycles of 95°C for 10 seconds, 60°C for 15 seconds, and 72 °C for 20 seconds. Primer sequences (Sigma-Aldrich, Gillingham, UK) for specific target genes are listed in Table 3. Glyceraldehyde-3-phosphate dehydrogenase (*GAPDH*) was used as the reference gene in each experiment. Relative quantification of mRNA levels of the target genes was analyzed using the comparative CT (threshold cycle) method ($2^{-\Delta\Delta Ct}$), as previously described by Livak et al. Relative expression levels were calculated for each sample after normalization against the reference gene. All experiments were performed four times in duplicate (n=8).

Table 3. Primers used for RT-qPCR.

Gene	Primer sequence (5′ to 3′) Forward	Primer sequence (5′ to 3′) Reverse
glyceraldehyde-3-phosphate dehydrogenase (*GAPDH*)	GAAGGTGAAGGTCGGAGTC	GAGATGGTGATGGGATTTC
RUNX family transcription factor 2 (*RUNX2*)	TCTTAGAACAAATTCTGCCCTTT	TGCTTTGGTCTTGAAATCACA
collagen type I alpha 1 chain (*COL1A1*)	GGTCAAGATGGTCGCCCC	GGAACACCTCGCTCTCCAG
alkaline phosphatase (*ALPL*)	CCTCGTTGACACCTGGAAGAG	TTCCGTGCGGTTCCAGA
osteopontin (*SPP1*)	CGAGGTGATAGTGTGGTTTATGG	GCACCATTCAACTCCTCGCTTTC
bone gamma-carboxyglutamate protein (*BGLAP*)	CTACCTGTATCAATGGCTGGG	GGATTGAGCTCACACACCT
interleukin-1 alpha (*IL1A*)	CGCCAATGACTCAGAGGAAGA	AGGGCGTCATTCAGGATGAA
interleukin-1 beta (*IL1B*)	TTCGAGGCACAAGGCACAA	AAGTCATCCTCATTGCCACTGT
interleukin-8 (*IL8*)	ATGACTTCCAA-GCTGGCCGTGGCT	TCTCAGCCCTCTTCAAAAACTTCT

2.11. Statistical analysis

Data are presented as mean values ± standard deviation (SD) or standard error of the mean (SEM). Statistical differences in the *in vitro* studies were calculated using one-way ANOVA, followed by a multiple comparison Bonferroni test, performed with SPSS version 22 (IBM, Armonk, NY, USA). A p value< 0.05 was considered statistically significant.

3. Results and Discussion

3.1. Characterization of the WPI/PG coatings on Ti6Al4V alloy

The presence of WPI/PG coatings on Ti was confirmed using XPS analyses. As shown in Figure 2, all coatings were mainly constituted of carbon (C), nitrogen (N), and oxygen (O) which demonstrates the presence of the protein layer. Indeed, nitrogen and carbon were detected from the protein containing primary amine (-NH2) and carboxyl (-COOH) functional groups. Moreover, the decrease in %Ti from 15% (uncoated Ti) to less than 4% confirmed the presence of the coating. As Ti signal was still detected in the presence of WPI fibrils, the coating may be either thinner than 15 nm which is the depth detection limit of XPS, or non-uniform revealing gaps between the fibrils. No significant differences were observed among the different coatings. However, the Ti content decreased significantly from 3.6% (WPI) to 0.4% ([WPI]autoclave + PG 0.5%) which indicates that the coating may be thinner or more uniform. PG was not easily detectable, as oxygen and carbon signals may come from both the protein and Ti substrate.

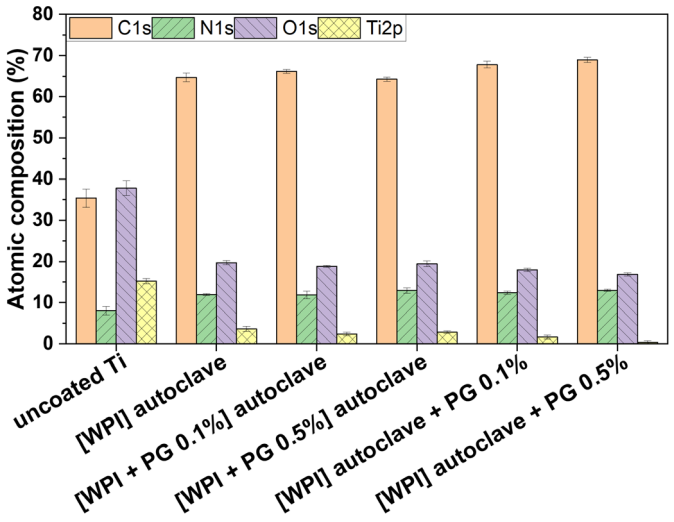

Figure 2. Atomic composition of uncoated Ti and WPI coatings without PG, with 0.1% of PG and 0.5% of PG. [WPI + PG 0.1%]autoclave and [WPI + PG 0.5%]autoclave mean that the coatings containing PG were autoclaved. [WPI]autoclave + PG 0.1% and [WPI]autoclave + PG 0.5% mean that only WPI coating was autoclaved, PG was added afterwards using a sterile filter and syringe. Error bars represent SD. Ti: titanium alloy Ti6Al4V; WPI: whey protein isolate; PG: phloroglucinol.

SEM images of coatings (Figure S1, Supplementary information) demonstrated the presence of fibrils and that fibrils withstood autoclaving, as demonstrated in previous work [21]. The presence of PG did not appear to influence fibril thickness, which was approximately 20 microns on all samples. The fibril layers appeared to be approximately 1 fibril thick and covered most of the sample surfaces, which is in agreement with the XPS results (Figure 2). As WPI fibrils are large molecules which withstand autoclaving and have a very high surface area/volume ratio, it is expected that the coatings will be stable under physiological conditions, in the same way that collagen fibril coatings are known to be stable. The fibril thicknesses observed in this study are consistent with those observed in previous work [24,27]. The fact that PG did not influence fibril thickness

suggests that it is not incorporated into fibrils during fibril formation and binds to the surface of already formed fibrils. Alternatively, if it is incorporated into fibrils, being a small molecule, its presence may not impede fibril formation, or does not significantly. This finding is similar to that observed in our previous work on collagen fibril coatings containing PG [23] where no marked change in morphology of collagen fibrils was observed due the presence of PG.

3.2. Characterization of the multispecies biofilm

The architecture of biofilm after 5 days of cultivation was assessed using scanning electron microscopy (SEM). As shown in Figure 3a the biofilm showed formation of 3D structure with spatial heterogeneity in bacterial arrangement. Co-aggregates of *P. gingivalis*, *A. actinomycetemcomitans*, *F. nucleatum*, and *S. mitis* were observed across the entire surface. These species were identified in the SEM micrograph based on their distinct morphological features: *S. mitis* appeared as spherical cells arranged in long chains, *F. nucleatum* as elongated and slender rods, *P. gingivalis* as short rods, and *A. actinomycetemcomitans* as small, oval-shaped coccobacilli [35–38].

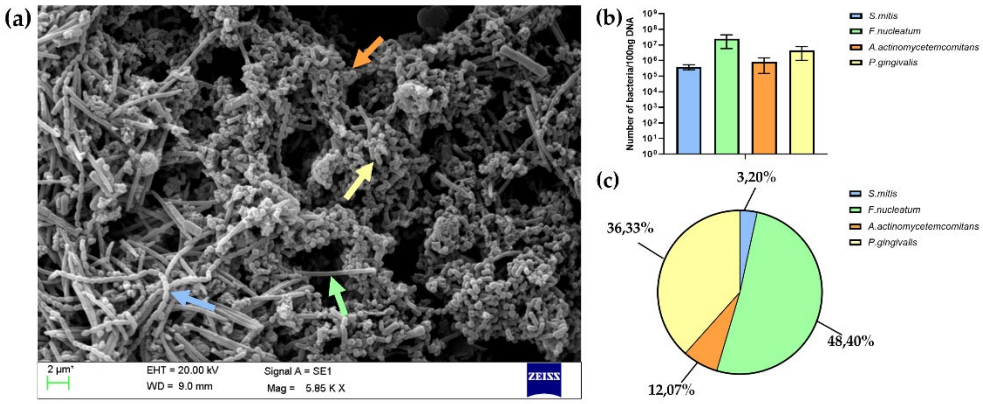

Figure 3. (**a**) Representative scanning electron micrograph of a multispecies biofilm formed on a glass coverslip, subsequently used in the co-culture model with BM-MSCs. Arrows in the SEM image indicate examples of four different bacterial species: *S. mitis* (blue arrow), *F. nucleatum* (green arrow), *P. gingivalis* (yellow arrow), and *A. actinomycetemcomitans* (orange arrow); (**b**) The number of each bacterial species quantified using the qPCR method and calculated per 100 ng of DNA isolated from the biofilm; (**c**) The results of bacterial quantification presented as the percentage (%) of the total number of bacteria in the biofilm.

Additionally, SEM analysis confirmed the presence of extracellular polymeric substances (EPS), which form a sticky matrix embedding the bacteria and contributing to biofilm stabilization. Quantification of each bacterial species in the mature biofilm was performed using qPCR method. The results presented in Figure 3b and 3c indicated the dominance of *F. nucleatum* within the mature biofilm, followed by *P. gingivalis*, with smaller contributions from *A. actinomycetemcomitans* and *S. mitis*. The obtained proportions of bacteria reflect the composition of pathogenic oral biofilm associated with peri-implant infections, where increases in the number of pathogenic bacteria, such as *F. nucleatum* and *P. gingivalis*, are observed along with a reduction in the number of *Streptococcus* species [3–5].

The established multispecies biofilm was subsequently used in an *in vitro* co-culture model with human BM-MSCs. In contrast to many previous studies focusing on single bacterial species or isolated virulence factors such as lipopolysaccharide (LPS) to mimic peri-implant infections, the present study employed a complex, multispecies biofilm that closely reflects the polymicrobial nature of peri-implantitis [31,39,40]. Using this model, WPI/PG coatings were evaluated for their potential to modulate the BM-MSC response under biofilm challenge. By incorporating these coatings into the co-culture model, the

study aimed to assess not only their osteogenic properties but also their ability to support BM-MSC function in the presence of a biofilm microenvironment.

3.3. In vitro studies: evaluation of WPI/PG coatings in a co-culture model of multispecies biofilm and BM-MSCs

In the present study osteogenic and anti-inflammatory properties of WPI/PG coatings on Ti were evaluated using BM-MSCs. These cells can undergo differentiation into multiple cell types and modulate host-immune responses by the secretion of pro-healing factors, including growth factors, cytokines and chemokines [41,42]. However, due to the presence of oral pathogenic biofilms, the integration of Ti implant with bone tissue can be affected [3]. Therefore, in this work, BM-MSCs were stimulated with multispecies biofilm to investigate the effect of the coatings on unstimulated and biofilm-stimulated cell behaviour.

3.3.1. BM-MSCs attachment, spreading and morphology

The implant surface determines the morphology of MSCs, which is a key indicator of cell adhesion and differentiation [43]. SEM images were obtained after 72 hours of BM-MSC culture to assess the differences in cell attachment, spreading, and morphology on uncoated Ti and WPI-coated Ti, with and without PG (Figure 4).

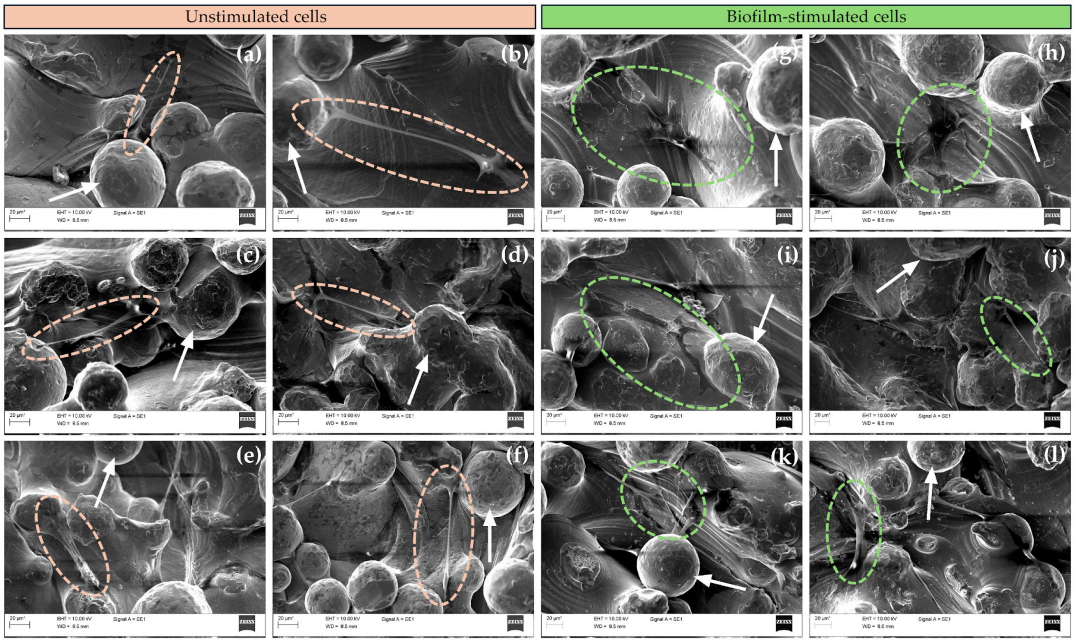

Figure 4. Representative SEM images of unstimulated and biofilm-stimulated BM-MSCs on (**a**), (**g**) uncoated Ti6Al4V; (**b**), (**h**) WPI, (**c**), (**i**) [WPI + PG 0.1%]autoclave; (**d**), (**j**) [WPI + PG 0.5%]autoclave; (**e**), (**k**) [WPI]autoclave + PG 0.1%, and (**f**), (**l**) [WPI]autoclave + PG 0.5% coatings on Ti6Al4V. Ellipses indicate unstimulated cells (orange) and biofilm-stimulated cells (green) and white arrows show particles of Ti6Al4V powder. Scale bar: 20 μm. Ti: titanium alloy Ti6Al4V; WPI: whey protein isolate; PG: phloroglucinol.

For all tested surfaces, BM-MSCs were located in the pores between the particles of Ti powder. Moreover, cells appeared to spread well on all coating types, showing elongated morphology and displaying numerous filopodia. No significant differences in cell morphology or spreading between the sample groups were observed. These results indicate that cell attachment, spreading, and morphology depend more on the topography of Ti discs than on the incorporated WPI coatings. Numerous studies have shown the positive effect of porous surfaces on cell adhesion [44,45], and our results clearly demonstrate that the cells adhered well to all porous Ti surfaces and developed numerous filopodia, indicating good affinity with the Ti, regardless of WPI coatings [46].

The morphology of BM-MSCs was also assessed in response to biofilm stimulation. After biofilm exposure, BM-MSCs cultured on uncoated Ti and WPI coatings without PG showed a more flattened morphology, whereas on WPI coatings enriched with different concentrations of PG, most cells demonstrated an elongated spindle shape, similar to the morphology observed in unstimulated BM-MSCs. These results suggest a possible protective role of PG incorporated into WPI coatings for BM-MSCs upon biofilm exposure. This observation is particularly relevant in the context of peri-implantitis, where local inflammation and bacterial colonization often compromise the regenerative potential of MSCs. The ability of PG-enriched WPI coatings to maintain the typical spindle-like morphology of BM-MSCs suggests a modulatory effect of these coatings on their response to biofilm-associated inflammation, potentially by limiting cytoskeletal rearrangements. Additionally, the flattened morphology observed under biofilm challenge in cells on uncoated Ti surfaces or those coated with PG-free WPI may reflect a stress-induced phenotype or an early sign of impaired function of BM-MSCs. It has been reported that a large, flat morphology is more typical of the inflammatory phenotype of BM-MSCs, while the spindle-shaped form corresponds to osteoblastic morphology [47]. The protective effect of PG may result from its antioxidant, anti-inflammatory, or antimicrobial properties [22].

Together, these results indicate that PG-enriched WPI coatings actively protect BM-MSC morphology under inflammatory conditions, helping maintain their regenerative capacity. This supports their potential as bioactive surface coatings to improve implant outcomes in peri-implantitis.

3.3.2. BM-MSCs metabolic activity

Metabolic activity of unstimulated and biofilm-stimulated BM-MSCs was assessed after 48 hours, as summarized in Figure 5.

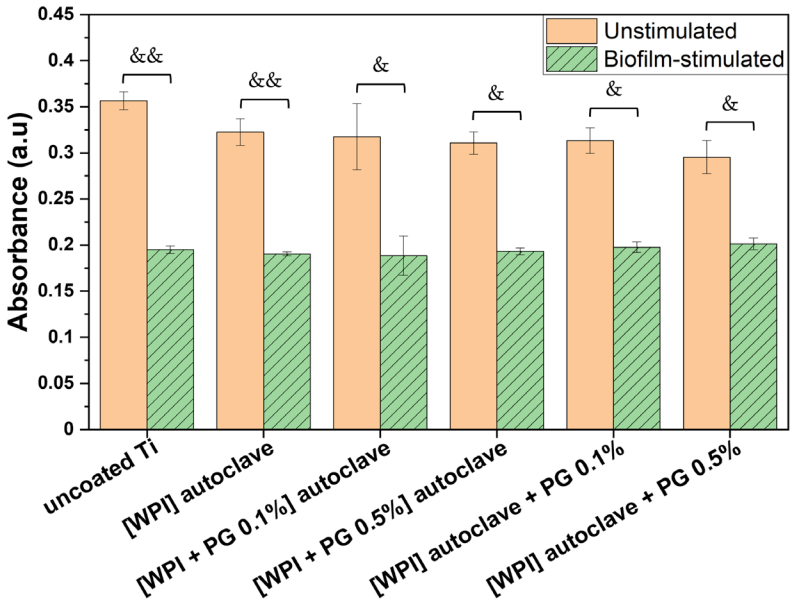

Figure 5. Metabolic activity of unstimulated and biofilm-stimulated BM-MSCs after 48 hours using MTT test. BM-MSCs were stimulated with biofilm for 2 hours and metabolic activity was analyzed directly after biofilm stimulation. The results are shown as mean (n = 4, two technical repetitions) and bars represent SEM. Significant differences for unstimulated vs. biofilm-stimulated BM-MSCs are indicated with & ($p<0.05$), and && ($p<0.01$). Ti: titanium alloy Ti6Al4V; WPI: whey protein isolate; PG: phloroglucinol.

The results showed a significant decrease in metabolic activity when cells had been stimulated with biofilm. This may be due to the release of soluble factors from the biofilm

which impact the cell function, as already mentioned in a previous study [48]. They showed that mesenchymal stromal cells exposed to *Staphylococcus aureus* and *Pseudomonas aeruginosa* biofilm media exhibited reduced cell viability due to apoptosis activation, as well as reduced migration and differentiation abilities. Other studies have investigated this effect, particularly in the context of chronic wounds, where biofilm is considered to contribute to wound chronicity [49].

Although biofilm stimulation led to reduced metabolic activity across all tested groups, the extent of the reduction varied depending on the surface. In the absence of biofilm, all surfaces—including uncoated Ti, WPI, and WPI enriched with either 0.1% or 0.5% PG—supported similarly high levels of metabolic activity, indicating that neither the WPI coating nor the addition of PG compromised BM-MSC viability. Upon biofilm exposure, the most pronounced reduction was observed on uncoated Ti (approximately 50% decrease), followed by WPI alone, which also showed a marked decrease. Interestingly, the WPI coatings supplemented with PG resulted in an attenuated decrease, indicating a protective effect. Notably, in the presence of 0.5% PG, biofilm-stimulated BM-MSCs exhibited a smaller decrease in metabolic activity compared to those cultured on 0.1% PG, indicating a dose-dependent effect. These findings suggest that PG not only maintains BM-MSC viability under normal conditions but may also mitigate biofilm-induced metabolic impairment.

3.3.3. Expression of genes related to bone matrix formation and mineralization in BM-MSCs

The gene expression of bone matrix formation markers was analyzed in unstimulated and biofilm-stimulated cells. Runt-related transcription factor 2 (*RUNX2*) is an early marker of bone matrix formation, as it is expressed in preosteoblast cells, while collagen type I alpha 1 chain (*COL1A1*) is known as a key marker of bone matrix production [50,51]. Both genes are important markers of the early stages of bone-implant integration. As illustrated in Figure 6a, the incorporation of PG into WPI coatings resulted in an up-regulation of *RUNX2* expression in unstimulated BM-MSCs. This finding is highly significant, as RUNX2 is considered the most important transcription factor in osteogenesis, playing a pivotal role in the early differentiation of BM-MSCs. Numerous studies have demonstrated that overexpression of *RUNX2* induces the differentiation of BM-MSCs into osteoblasts and activates osteogenesis-related genes such as collagen type I, osteopontin, and bone gamma-carboxyglutamate protein [52,53]. Our results indicate that WPI/PG coatings promote the osteogenic differentiation of BM-MSCs by up-regulating *RUNX2* expression. However, elevated expression of *RUNX2* can inhibit cell proliferation by promoting cell-cycle arrest in the G0/G1 phase [52]. MTT results (Figure 5), which reflect both metabolic activity and cell proliferation, showed that WPI/PG coatings slightly reduced BM-MSC proliferation, but the differences were not statistically significant. This suggests that PG incorporation into WPI coatings, at the tested concentrations, can significantly enhance BM-MSC differentiation without impairing proliferation.

RT-qPCR analysis of *COL1A1* expression further confirmed the pro-osteogenic potential of PG-enriched WPI coatings. A significant up-regulation of *COL1A1* was observed in BM-MSCs cultured on these coatings, with expression levels positively correlating with the concentration of PG (Figure 6b). These results are in accordance with our previous study on PG incorporated into collagen fibrillar coatings, where *COL1A1* expression was also studied [23]. Notably, the highest *COL1A1* expression was detected in cells grown on coatings containing the highest amount of PG without being autoclaved. This indicates that PG was more biologically active without being sterilized by autoclaving and the heat may impact its activity.

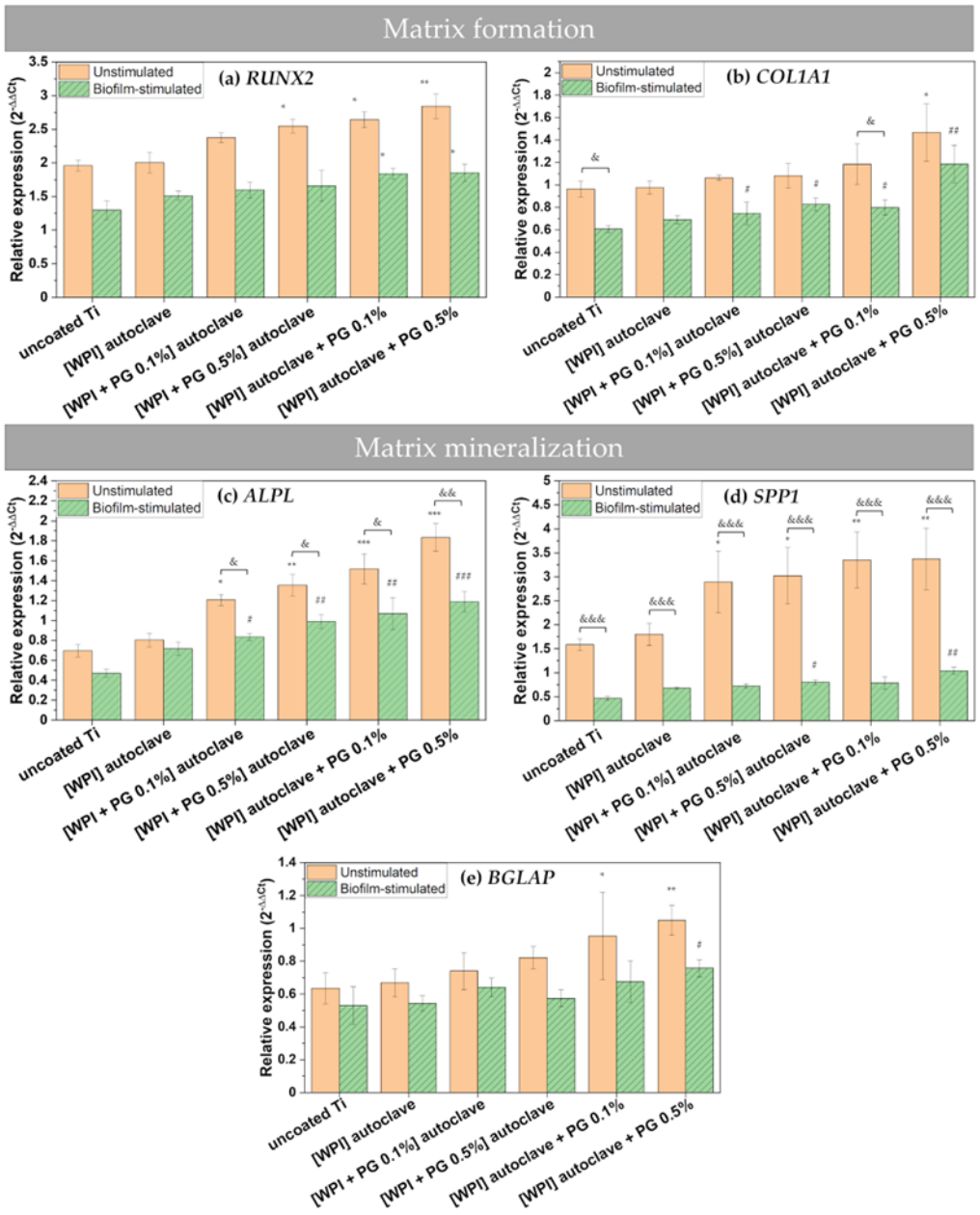

Figure 6. Relative gene expression for matrix formation markers: (a*) RUNX2*, and (b) *COL1A1* and matrix mineralization markers: (a) *ALPL*, (b) *SPP1*, and (c) *BGLAP*. The results are shown as mean (n = 4, two technical repetitions) and bars represent SEM. * and # represent statistical analyses between uncoated Ti and tested samples for unstimulated cells and biofilm-stimulated cells, respectively. (*,#, & p<0.05; **, ##, && p<0.01; ***, ###, &&& p<0.001). Ti: titanium alloy Ti6Al4V; WPI: whey protein isolate; PG: phloroglucinol.

Other studies have also indicated that the addition of PG into WPI hydrogels supports the growth and collagen production of human dental pulp stem cells (DPSCs), promoting the formation of the ECM [19]. Given that COL1A1 is an abundant protein in the native ECM and plays a crucial role in maintaining the structural integrity of newly formed bone, our findings highlight the potential of WPI/PG coatings to support early matrix deposition. Moreover, the observed increase in *COL1A1* expression may be directly linked to higher *RUNX2* levels, as RUNX2 is known to regulate the transcription of *COL1A1* [53]. Together, these results point to a synergistic effect of WPI/PG coatings in enhancing osteogenic differentiation and matrix formation, which is essential for successful bone–implant integration.

As shown in Figure 6a, biofilm stimulation significantly down-regulated the expression of *RUNX2* on all examined Ti surfaces. The expression of *COL1A1* also appeared to be reduced in biofilm-stimulated cells compared to unstimulated cells, but the differences were not statistically significant (Figure 6b). Notably, in the presence of PG-enriched WPI coatings, the expression of these genes in biofilm-stimulated cells increased compared to uncoated Ti, particularly when PG was not autoclaved and was present at a concentration of 0.5%. These findings suggest that PG-enriched WPI coatings may help maintain osteogenic potential even under peri-implantitis-like conditions.

Persistent colonization of implant surfaces by pathogenic bacteria can strongly inhibit the osteogenic differentiation of BM-MSCs [39]. However, based on *RUNX2* and *COL1A1* expression profiles in infected BM-MSCs, WPI/PG coatings could sustainably promote osteogenic differentiation even during infection. Future studies should examine whether WPI/PG coatings reduce matrix metalloproteinase (MMP) expression in infected BM-MSCs, since elevated MMPs, particularly those degrading collagen I and III, impair bone-matrix formation [54]. Thus, reducing MMP level could prevent matrix breakdown and support regeneration upon peri-implantitis.

Here, we investigated also the effect of PG-enriched WPI coatings on the mineralization potential of BM-MSCs by measuring the gene expression of osteogenic markers. The results showed that WPI coatings with PG promoted the mRNA expression of alkaline phosphatase (*ALPL*), osteopontin (*SPP1*), and bone gamma-carboxyglutamate protein (*BGLAP*) in both unstimulated and biofilm-stimulated cells. These findings are important, as *ALPL* is an essential marker for bone mineralization of osteoblastic cells [55], *SPP1* is a key marker of osteogenic differentiation [56], and *BGLAP* is involved in the regulation of the mineralization process [57].

The expression of all osteogenic genes increased in the presence of PG. Similar results were observed in our previous study on PG using human osteosarcoma cell line SaOS-2, where the gene expression of osteogenic markers was evaluated [23]. Moreover, our findings demonstrate a clear, dose-dependent pro-osteogenic activity of PG. Without biofilm stimulation, 0.5 % PG caused the most pronounced induction of *ALPL* and *SPP1* (Figure 6c–d), whereas the effect on the late marker *BGLAP* was more limited, but still significant. This attenuated response is likely due to the early measurement time point (day 3), as *BGLAP* typically peaks between days 14 and 21 in osteoblast-lineage cultures, so the capacity of WPI/PG coatings to up-regulate this late marker may be under-represented here [58,59]. Incorporating PG after autoclaving further enhanced osteogenic responses, implying that heat reduces but does not eliminate PG activity.

Biofilm stimulation markedly reduced osteogenic gene expression—particularly *SPP1*—on all Ti surfaces. Nevertheless, PG-enriched WPI coatings, especially the non-autoclaved 0.5 % PG variant, maintained elevated *ALPL* expression under biofilm stimulation, indicating that PG/WPI coatings form a protective interface that preserves osteogenic activity despite microbial challenge. Up-regulation of osteogenic markers in both unstimulated and biofilm-stimulated BM-MSCs aligns with increased *RUNX2* levels: PG increases *RUNX2*, which then activates its downstream transcriptional targets, first driving matrix deposition (*COL1A1*) and later mineralization (*ALPL*, *SPP1*, *BGLAP*).

Overall, the results suggest that PG-enriched WPI coatings on titanium may promote bone formation and mineralization by enhancing the expression of osteogenic markers, even in the presence of implant-related biofilm infection. The enhanced osteogenesis observed in response to PG-enriched WPI coatings could potentially improve bone-implant integration and reduce the risk of implant failure. However, WPI/PG coatings may alter surface properties, such as roughness, which may also contribute to the increased expression of osteogenic markers. Therefore, future studies should provide a detailed physicochemical characterization of these properties and correlate them with the *in vitro* results to clarify how each parameter contributes to the observed pro-osteogenic effect.

3.3.4. Gene expression of pro-inflammatory markers in BM-MSCs

The implantation of biomaterials, such as Ti implants, into bone may trigger host responses, including excessive inflammation, which can interfere with the bone healing process. Notably, the secretion of inflammatory cytokines is not restricted to immune cells alone. MSCs recruited to the implantation site are also capable of producing a broad range of cytokines, including interleukins, which are involved in the regulation of inflammation and osteogenesis [60]. In this study, the gene expression of selected pro-inflammatory markers, interleukin-1α (*IL1A*), interleukin-1β (*IL1B*), and interleukin-8 (*IL8*), was evaluated, as shown in Figure 7.

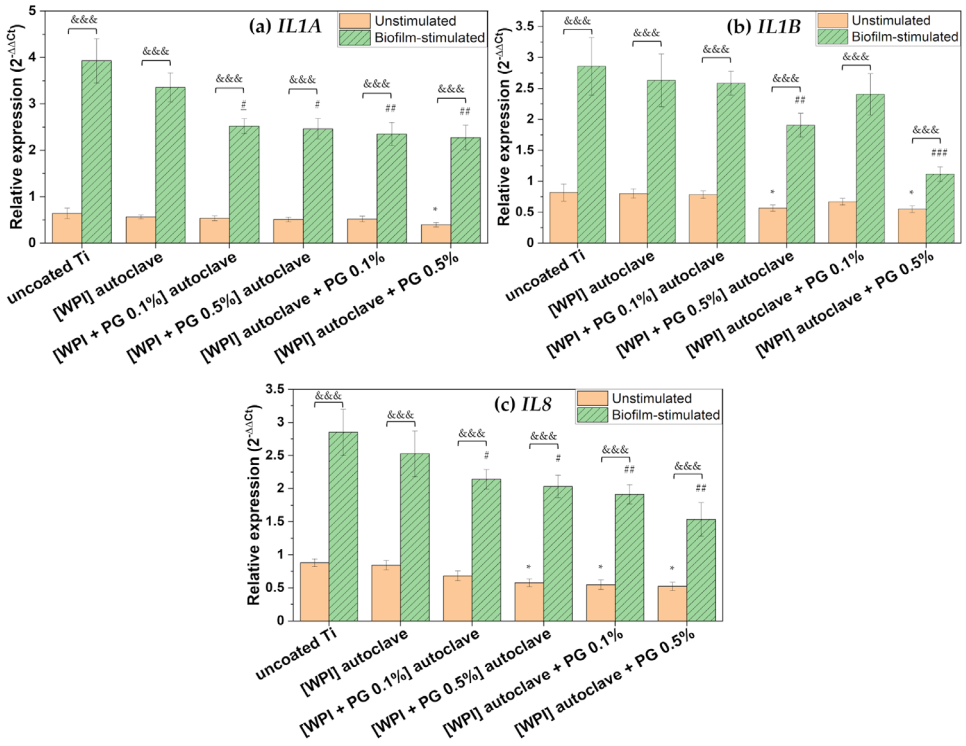

Figure 7. Relative gene expression of pro-inflammatory markers: (a) *IL1A*, (b) *IL1B*, and (c) *IL8*. The results are shown as mean (n = 4, two technical repetitions) and bars represent SEM. * and # represent significant differences between uncoated Ti and tested samples for unstimulated cells and biofilm-stimulated cells, respectively. (*, # $p<0.05$; ##, && $p<0.01$; ###, &&& $p<0.001$). Ti: titanium alloy Ti6Al4V; WPI: whey protein isolate; PG: phloroglucinol.

WPI containing PG exhibited a general significant down-regulation of pro-inflammatory markers in unstimulated BM-MSCs compared to uncoated Ti. Moreover, the results indicated that WPI coatings containing a high amount of PG (0.5%) added after autoclaving down-regulated the gene expression of *IL1B* and *IL8*, suggesting that PG-enriched WPI coatings may contribute to the attenuation of the inflammatory response.

IL-8 plays a pivotal role in the recruitment of neutrophils to the site of implantation [61]. Although neutrophils are essential during the early stages of healing, their prolonged activation, especially under continuous stimulation by microbial factors, can lead to the release of MMPs and other degradative enzymes that contribute to bone damage and may compromise implant integration [54]. The observed down-regulation of *IL8* in BM-MSCs cultured on WPI/PG-coated surfaces may therefore reflect a reduction in neutrophil chemoattractant signaling, potentially mitigating excessive inflammation. IL-1β is also a key mediator of inflammation that has been associated with bone resorption and impaired osteogenic differentiation of MSCs. High and persistent expression of *IL1B* at the implant site inhibits osteogenesis, stimulates osteoclastogenesis, and disrupts implant integration. Therefore, the reduced expression of *IL1B* in response to WPI/PG coatings is significant,

as it may contribute to a more favorable inflammatory environment for bone-implant integration. Importantly, this suppressive effect on *IL1B* was observed only in the presence of PG, as WPI coatings alone did not induce any changes. Furthermore, the inhibitory effect was evident at the higher PG concentration of 0.5%, while the lower concentration of 0.1% did not affect *IL1B* expression. As already described in the literature, PG may prevent inflammation by down-regulating the gene expression of inflammatory markers, such as TNF-α, IL-1β, IL-6, and prostaglandin E_2, through a potential reaction mechanism between hydroxyl groups and reactive oxygen species [21]. These findings are in line with our previous study, where a similar anti-inflammatory effect of PG was observed on collagen fibrillar coatings [23].

No significant change in *IL1A* expression was observed in unstimulated BM-MSCs, suggesting that PG's immunomodulatory action could be selective.

As shown in Figure 7, BM-MSCs showed high expression of pro-inflammatory markers in response to oral bacterial biofilm challenge. Numerous studies have reported that complex multispecies biofilms stimulate various types of cells involved in bone-implant integration to express and release a variety of inflammatory mediators, including IL-1β, IL-6, and IL-8 [34,62,63]. The higher expression of these inflammatory mediators during biofilm-related peri-implant infections contributes to both soft and hard tissue damage [3,64]. In the present study, the bacterial biofilm used to challenge BM-MSCs was dominated by *F. nucleatum* and *P. gingivalis*, as shown in Figure 3. These bacteria are known to produce a range of virulence factors, including proteolytic enzymes, which are released into the culture medium and may strongly stimulate a pro-inflammatory response in BM-MSCs [31]. However, our results indicated that WPI coatings enriched with PG significantly reduced the expression of key pro-inflammatory markers in BM-MSCs challenged with biofilm. A marked downregulation of *IL1A* was observed on PG/WPI-coated surfaces—regardless of PG concentration—compared to uncoated Ti. Interestingly, this effect was not observed in unstimulated BM-MSCs, likely due to low basal *IL1A* expression, which possibly makes PG's effect undetectable without pro-inflammatory stimulation.

Moreover, PG incorporation into WPI coatings resulted in a dose-dependent decrease in the expression of *IL1B* and *IL8*, with the 0.5% PG concentration showing a more pronounced inhibitory effect than the 0.1% concentration. This finding is particularly relevant, as IL-1β is a well-recognized marker of peri-implantitis and is frequently detected at high levels in peri-implant crevicular fluid. Similarly, IL-8 is known to contribute to the pro-inflammatory environment at the implant surface, promoting osteoclast differentiation eventually accelerating bone resorption and compromising implant stability [65,66].

Importantly, our results also demonstrated that autoclaving PG could compromises its immunomodulatory properties. In the case of *IL1B* and *IL8*, coatings containing heat-sterilized PG exhibited reduced ability to suppress pro-inflammatory marker expression, indicating a possible thermal degradation of PG functional groups, which may impair its bioactivity. Therefore, non-thermal sterilization methods should be considered to maintain its biological function.

Taken together, these findings suggest that PG-enriched WPI coatings may help attenuate biofilm-induced inflammation by downregulating key mediators such as *IL1A*, *IL1B*, and *IL8*. This anti-inflammatory effect appears to be dose-dependent and to occur primarily under inflammatory conditions.

Furthermore, given that phenolic compounds like PG exhibit broad-spectrum antimicrobial activity [67–69], it is possible that the reduced inflammatory response observed here may also be partially attributed to antimicrobial effects. Future studies should evaluate the antibacterial properties of WPI/PG coatings and include protein-level analyses, such as quantitative proteomics, to better explain the mechanisms underlying their anti-inflammatory activity.

3.4. General discussion and Outlook

Further work should focus on adhesion studies and possible protein release from coatings, as well as possible effects of autoclaving on adhesion or protein release. Another future research topic is a comparison of PG with other bioactive molecules of plant origin, such as flavonoids, tannins or other polyphenols.

4. Conclusions

This study demonstrated that surface modification of Ti6Al4V alloy with WPI/PG coatings effectively enhances the interaction between BM-MSCs and titanium, even in the presence of pathogenic multispecies biofilms. Surprisingly, despite biofilm stimulation, BM-MSCs maintained strong adhesion properties and spindle-like morphology, particularly on PG-enriched WPI coatings. The metabolic activity of the cells in contact with WPI/PG coatings remained unchanged, indicating good biocompatibility. Furthermore, WPI/PG coatings promoted the expression of key osteogenic markers, facilitating enhanced bone formation and mineralization, especially with 0.5% PG added after autoclaving. Additionally, these coatings significantly reduced the expression of pro-inflammatory markers, highlighting their anti-inflammatory potential. In conclusion, our findings suggest that WPI/PG coatings can not only improve bone-implant integration but also reduce inflammation in biofilm-prone environments, offering an inexpensive and promising strategy for orthopedic and dental implant applications. However, further studies are needed to fully explore their antimicrobial potential.

Funding: This research was funded by the Engineering and Physical Sciences Research Council (EPSRC) "A novel coating technology based upon polyatomic ions from plasma", grant number EP/S004505/1

Institutional Review Board Statement: Not applicable.

Data Availability Statement: The original contributions presented in this study are included in the article. Further inquiries can be directed to the corresponding author.

Acknowledgments: The authors would like to acknowledge Alexander Robson for his assistance with XPS analyses.

Conflicts of Interest: The authors declare no conflicts of interest. The funders had no role in the design of the study; in the collection, analyses, or interpretation of data; in the writing of the manuscript; or in the decision to publish the results.

References

1. Ma, Y.; Wang, S.; Wang, H.; Chen, X.; Shuai, Y.; Wang, H.; Mao, Y.; He, F. Mesenchymal Stem Cells and Dental Implant Osseointegration during Aging: From Mechanisms to Therapy. *Stem Cell Res. Ther.* **2023**, *14*, 382, doi:10.1186/s13287-023-03611-
2. Emam, S.M.; Moussa, N. Signaling Pathways of Dental Implants' Osseointegration: A Narrative Review on Two of the Most Relevant; NF-κB and Wnt Pathways. *BDJ Open* **2024**, *10*, 29, doi:10.1038/s41405-024-00211-w.
3. Lasserre, J.F.; Brecx, M.C.; Toma, S. Oral Microbes, Biofilms and Their Role in Periodontal and Peri-Implant Diseases. *Materials* **2018**, *11*, 1802, doi:10.3390/ma11101802.
4. Seo, B.Y.; Son, K.; Son, Y.-T.; Dahal, R.H.; Kim, S.; Kim, J.; Hwang, J.; Kwon, S.-M.; Lee, J.-M.; Lee, K.-B.; et al. Influence of Dental Titanium Implants with Different Surface Treatments Using Femtosecond and Nanosecond Lasers on Biofilm Formation. *J. Funct. Biomater.* **2023**, *14*, 297, doi:10.3390/jfb14060297.
5. Kligman, S.; Ren, Z.; Chung, C.-H.; Perillo, M.A.; Chang, Y.-C.; Koo, H.; Zheng, Z.; Li, C. The Impact of Dental Implant Surface Modifications on Osseointegration and Biofilm Formation. *J. Clin. Med.* **2021**, *10*, 1641, doi:10.3390/jcm10081641.
6. Zhao, H.; Yang, Y.; An, J.; Xin, H.; Xiao, Y.; Jia, Z.; Wu, Y.; Sheng, L.; Wen, M. Cu2 O Nanocubes Embedded in Polycaprolactone Nanofibers for Photo–Chemotherapeutic Wound Disinfection and Regeneration. ACS Appl. Nano Mater. 2024, 7, 17707–17718, doi:10.1021/acsanm.4c02928.
7. Nazarov, D.; Kozlova, L.; Rogacheva, E.; Kraeva, L.; Maximov, M. Atomic Layer Deposition of Antibacterial Nanocoatings: A Review. Antibiotics 2023, 12, 1656, doi:10.3390/antibiotics12121656.
8. Long, L.; Fan, Y.; Yang, X.; Ding, X.; Hu, Y.; Zhang, G.; Xu, F.-J. A Hydrophobic Cationic Polyphenol Coating for Versatile Antibacterial and Hemostatic Devices. Chem. Eng. J. 2022, 444, 135426, doi:10.1016/j.cej.2022.135426.

9. Malheiros, S.S.; Nagay, B.E.; Bertolini, M.M.; De Avila, E.D.; Shibli, J.A.; Souza, J.G.S.; Barão, V.A.R. Biomaterial Engineering Surface to Control Polymicrobial Dental Implant-Related Infections: Focusing on Disease Modulating Factors and Coatings Development. *Expert Rev. Med. Devices* **2023**, *20*, 557–573, doi:10.1080/17434440.2023.2218547.
10. Douglas, T.E.L.; Vandrovcová, M.; Kročilová, N.; Keppler, J.K.; Zárubová, J.; Skirtach, A.G.; Bačáková, L. Application of Whey Protein Isolate in Bone Regeneration: Effects on Growth and Osteogenic Differentiation of Bone-Forming Cells. *J. Dairy Sci.* **2018**, *101*, 28–36, doi:10.3168/jds.2017-13119.
11. Heyn, T.R.; Garamus, V.M.; Neumann, H.R.; Uttinger, M.J.; Guckeisen, T.; Heuer, M.; Selhuber-Unkel, C.; Peukert, W.; Keppler, J.K. Influence of the Polydispersity of pH 2 and pH 3.5 Beta-Lactoglobulin Amyloid Fibril Solutions on Analytical Methods. *Eur. Polym. J.* **2019**, *120*, 109211, doi:10.1016/j.eurpolymj.2019.08.038.
12. Akkermans, C.; Venema, P.; Van Der Goot, A.J.; Gruppen, H.; Bakx, E.J.; Boom, R.M.; Van Der Linden, E. Peptides Are Building Blocks of Heat-Induced Fibrillar Protein Aggregates of β-Lactoglobulin Formed at pH 2. *Biomacromolecules* **2008**, *9*, 1474–1479, doi:10.1021/bm7014224.
13. Keppler, J.K.; Martin, D.; Garamus, V.M.; Berton-Carabin, C.; Nipoti, E.; Coenye, T.; Schwarz, K. Functionality of Whey Proteins Covalently Modified by Allyl Isothiocyanate. Part 1 Physicochemical and Antibacterial Properties of Native and Modified Whey Proteins at pH 2 to 7. *Food Hydrocoll.* **2017**, *65*, 130–143, doi:10.1016/j.foodhyd.2016.11.016.
14. Gupta, D.; Kocot, M.; Tryba, A.M.; Serafim, A.; Stancu, I.C.; Jaegermann, Z.; Pamuła, E.; Reilly, G.C.; Douglas, T.E.L. Novel Naturally Derived Whey Protein Isolate and Aragonite Biocomposite Hydrogels Have Potential for Bone Regeneration. *Mater. Des.* **2020**, *188*, 108408, doi:10.1016/j.matdes.2019.108408.
15. Hempel, U.; Matthäus, C.; Preissler, C.; Möller, S.; Hintze, V.; Dieter, P. Artificial Matrices With High-Sulfated Glycosaminoglycans and Collagen Are Anti-Inflammatory and Pro-Osteogenic for Human Mesenchymal Stromal Cells. *J. Cell. Biochem.* **2014**, *115*, 1561–1571, doi:10.1002/jcb.24814.
16. Hempel, U.; Preissler, C.; Vogel, S.; Möller, S.; Hintze, V.; Becher, J.; Schnabelrauch, M.; Rauner, M.; Hofbauer, L.C.; Dieter, P. Artificial Extracellular Matrices with Oversulfated Glycosaminoglycan Derivatives Promote the Differentiation of Osteoblast-Precursor Cells and Premature Osteoblasts. *BioMed Res. Int.* **2014**, *2014*, 1–10, doi:10.1155/2014/938368.
17. Norris, K.; Kocot, M.; Tryba, A.M.; Chai, F.; Talari, A.; Ashton, L.; Parakhonskiy, B.V.; Samal, S.K.; Blanchemain, N.; Pamuła, E.; et al. Marine-Inspired Enzymatic Mineralization of Dairy-Derived Whey Protein Isolate (WPI) Hydrogels for Bone Tissue Regeneration. *Mar. Drugs* **2020**, *18*, 294, doi:10.3390/md18060294.
18 Lee, Dae-Sung; Cho, Young-Sook; Je, Jae-Young Antioxidant and Antibacterial Activities of Chitosan-Phloroglucinol Conjugate. *Fish. Aquat. Sci.* **2013**, *16*, 229–235, doi:10.5657/FAS.2013.0229.
19. Platania, V.; Douglas, T.E.L.; Zubko, M.K.; Ward, D.; Pietryga, K.; Chatzinikolaidou, M. Phloroglucinol-Enhanced Whey Protein Isolate Hydrogels with Antimicrobial Activity for Tissue Engineering. *Mater. Sci. Eng. C* **2021**, *129*, 112412, doi:10.1016/j.msec.2021.112412.
20. Kang, K.A.; Lee, K.H.; Chae, S.; Zhang, R.; Jung, M.S.; Ham, Y.M.; Baik, J.S.; Lee, N.H.; Hyun, J.W. Cytoprotective Effect of Phloroglucinol on Oxidative Stress Induced Cell Damage via Catalase Activation. *J. Cell. Biochem.* **2006**, *97*, 609–620, doi:10.1002/jcb.20668
21. Kim, M.-M.; Kim, S.-K. Effect of Phloroglucinol on Oxidative Stress and Inflammation. *Food Chem. Toxicol.* **2010**, *48*, 2925–2933, doi:10.1016/j.fct.2010.07.029.
22. Lišková, J.; Douglas, T.E.L.; Beranová, J.; Skwarczyńska, A.; Božič, M.; Samal, S.K.; Modrzejewska, Z.; Gorgieva, S.; Kokol, V.; Bačáková, L. Chitosan Hydrogels Enriched with Polyphenols: Antibacterial Activity, Cell Adhesion and Growth and Mineralization. *Carbohydr. Polym.* **2015**, *129*, 135–142, doi:10.1016/j.carbpol.2015.04.043.
23. Mieszkowska, A.; Beaumont, H.; Martocq, L.; Koptyug, A.; Surmeneva, M.A.; Surmenev, R.A.; Naderi, J.; Douglas, T.E.L.; Gurzawska-Comis, K.A. Phenolic-Enriched Collagen Fibrillar Coatings on Titanium Alloy to Promote Osteogenic Differentiation and Reduce Inflammation. *Int. J. Mol. Sci.* **2020**, *21*, 6406, doi:10.3390/ijms21176406.
24. Rabe, R.; Hempel, U.; Martocq, L.; Keppler, J.K.; Aveyard, J.; Douglas, T.E.L. Dairy-Inspired Coatings for Bone Implants from Whey Protein Isolate-Derived Self-Assembled Fibrils. *Int. J. Mol. Sci.* **2020**, *21*, 5544, doi:10.3390/ijms21155544.
25. Douglas, T.E.L.; Hempel, U.; Żydek, J.; Vladescu, A.; Pietryga, K.; Kaeswurm, J.A.H.; Buchweitz, M.; Surmenev, R.A.; Surmeneva, M.A.; Cotrut, C.M.; et al. Pectin Coatings on Titanium Alloy Scaffolds Produced by Additive Manufacturing: Promotion of Human Bone Marrow Stromal Cell Proliferation. Mater. Lett. 2018, 227, 225–228, doi:10.1016/j.matlet.2018.05.060.
26. Van Bael, S.; Chai, Y.C.; Truscello, S.; Moesen, M.; Kerckhofs, G.; Van Oosterwyck, H.; Kruth, J.-P.; Schrooten, J. The Effect of Pore Geometry on the in Vitro Biological Behavior of Human Periosteum-Derived Cells Seeded on Selective Laser-Melted Ti6Al4V Bone Scaffolds. Acta Biomater. 2012, 8, 2824–2834, doi:10.1016/j.actbio.2012.04.001.
27. Facchetti, D.; Hempel, U.; Martocq, L.; Smith, A.M.; Koptyug, A.; Surmenev, R.A.; Surmeneva, M.A.; Douglas, T.E.L. Heparin Enriched-WPI Coating on Ti6Al4V Increases Hydrophilicity and Improves Proliferation and Differentiation of Human Bone Marrow Stromal Cells. Int. J. Mol. Sci. 2021, 23, 139, doi:10.3390/ijms23010139.
28. Keppler, J.K.; Heyn, T.R.; Meissner, P.M.; Schrader, K.; Schwarz, K. Protein Oxidation during Temperature-Induced Amyloid Aggregation of Beta-Lactoglobulin. *Food Chem.* **2019**, *289*, 223–231, doi:10.1016/j.foodchem.2019.02.114.
29. Surmeneva, M.; Chudinova, E.; Syrtanov, M.; Koptioug, A.; Surmenev, R. Investigation of the HA Film Deposited on the Porous Ti6Al4V Alloy Prepared via Additive Manufacturing. *IOP Conf. Ser. Mater. Sci. Eng.* **2015**, *98*, 012025, doi:10.1088/1757-899X/98/1/012025.

30. Norris, K.; Mishukova, O.I.; Zykwinska, A.; Colliec-Jouault, S.; Sinquin, C.; Koptioug, A.; Cuenot, S.; Kerns, J.G.; Surmeneva, M.A.; Surmenev, R.A.; et al. Marine Polysaccharide-Collagen Coatings on Ti6Al4V Alloy Formed by Self-Assembly. *Micromachines* **2019**, *10*, 68, doi:10.3390/mi10010068.
31. Ramage, G.; Lappin, D.F.; Millhouse, E.; Malcolm, J.; Jose, A.; Yang, J.; Bradshaw, D.J.; Pratten, J.R.; Culshaw, S. The Epithelial Cell Response to Health and Disease Associated Oral Biofilm Models. *J. Periodontal Res.* **2017**, *52*, 325–333, doi:10.1111/jre.12395.
32. Muchova, M.; Balacco, D.L.; Grant, M.M.; Chapple, I.L.C.; Kuehne, S.A.; Hirschfeld, J. Fusobacterium Nucleatum Subspecies Differ in Biofilm Forming Ability in Vitro. *Front. Oral Health* **2022**, *3*, 853618, doi:10.3389/froh.2022.853618.
33. Millhouse, E.; Jose, A.; Sherry, L.; Lappin, D.F.; Patel, N.; Middleton, A.M.; Pratten, J.; Culshaw, S.; Ramage, G. Development of an in Vitroperiodontal Biofilm Model for Assessing Antimicrobial and Host Modulatory Effects of Bioactive Molecules. *BMC Oral Health* **2014**, *14*, 80, doi:10.1186/1472-6831-14-80.
34. Guggenheim, B.; Gmür, R.; Galicia, J.C.; Stathopoulou, P.G.; Benakanakere, M.R.; Meier, A.; Thurnheer, T.; Kinane, D.F. In Vitromodeling of Host-Parasite Interactions: The "subgingival" Biofilm Challenge of Primary Human Epithelial Cells. *BMC Microbiol.* **2009**, *9*, 280, doi:10.1186/1471-2180-9-280.
35. Abranches, J.; Zeng, L.; Kajfasz, J.K.; Palmer, S.R.; Chakraborty, B.; Wen, Z.T.; Richards, V.P.; Brady, L.J.; Lemos, J.A. Biology of Oral Streptococci. Microbiol. Spectr. 2018, 6, 6.5.11, doi:10.1128/microbiolspec.GPP3-0042-2018.
36. Shahoumi, L.A.; Saleh, M.H.A.; Meghil, M.M. Virulence Factors of the Periodontal Pathogens: Tools to Evade the Host Immune Response and Promote Carcinogenesis. Microorganisms 2023, 11, 115, doi:10.3390/microorganisms11010115.
37. Chopra, A.; Bhat, S.G.; Sivaraman, K. Porphyromonas Gingivalis Adopts Intricate and Unique Molecular Mechanisms to Survive and Persist within the Host: A Critical Update. J. Oral Microbiol. 2020, 12, 1801090, doi:10.1080/20002297.2020.1801090.
38. Raja, M. Aggregatibacter Actinomycetemcomitans – A Tooth Killer? J. Clin. Diagn. Res. 2014, doi:10.7860/JCDR/2014/9845.4766.
39. Xing, H.; Taguchi, Y.; Komasa, S.; Yamawaki, I.; Sekino, T.; Umeda, M.; Okazaki, J. Effect of Porphyromonas Gingivalis Lipopolysaccharide on Bone Marrow Mesenchymal Stem Cell Osteogenesis on a Titanium Nanosurface. J. Periodontol. 2015, 86, 448–455, doi:10.1902/jop.2014.140386.
40. Huang, Z.; Chen, G.; Wu, H.; Huang, X.; Xu, R.; Deng, F.; Li, Y. Ebselen Restores Peri-Implantitis-Induced Osteogenic Inhibition via Suppressing BMSCs Ferroptosis. Exp. Cell Res. 2023, 427, 113612, doi:10.1016/j.yexcr.2023.113612.
41. Bifari, F.; Lisi, V.; Mimiola, E.; Pasini, A.; Krampera, M. Immune Modulation by Mesenchymal Stem Cells. *Transfus. Med. Hemotherapy* **2008**, *35*, 194–204, doi:10.1159/000128968.
42. Wang, M.; Yuan, Q.; Xie, L. Mesenchymal Stem Cell-Based Immunomodulation: Properties and Clinical Application. *Stem Cells Int.* **2018**, *2018*, 1–12, doi:10.1155/2018/3057624.
43. Boyan, B.D.; Cheng, A.; Olivares-Navarrete, R.; Schwartz, Z. Implant Surface Design Regulates Mesenchymal Stem Cell Differentiation and Maturation. *Adv. Dent. Res.* **2016**, *28*, 10–17, doi:10.1177/0022034515624444.
44. Civantos, A.; Domínguez, C.; Pino, R.J.; Setti, G.; Pavón, J.J.; Martínez-Campos, E.; Garcia Garcia, F.J.; Rodríguez, J.A.; Allain, J.P.; Torres, Y. Designing Bioactive Porous Titanium Interfaces to Balance Mechanical Properties and in Vitro Cells Behavior towards Increased Osseointegration. *Surf. Coat. Technol.* **2019**, *368*, 162–174, doi:10.1016/j.surfcoat.2019.03.001.
45. Yao, Y.; Yang, Y.; Ye, Q.; Cao, S.; Zhang, X.; Zhao, K.; Jian, Y. Effects of Pore Size and Porosity on Cytocompatibility and Osteogenic Differentiation of Porous Titanium. *J. Mater. Sci. Mater. Med.* **2021**, *32*, 72, doi:10.1007/s10856-021-06548-0.
46. Guadarrama Bello, D.; Fouillen, A.; Badia, A.; Nanci, A. A Nanoporous Titanium Surface Promotes the Maturation of Focal Adhesions and Formation of Filopodia with Distinctive Nanoscale Protrusions by Osteogenic Cells. *Acta Biomater.* **2017**, *60*, 339–349, doi:10.1016/j.actbio.2017.07.022.
47. Stone, A.P.; Rand, E.; Thornes, G.; Kay, A.G.; Barnes, A.L.; Hitchcock, I.S.; Genever, P.G. Extracellular Matrices of Stromal Cell Subtypes Regulate Phenotype and Contribute to the Stromal Microenvironment in Vivo. Stem Cell Res. Ther. 2024, 15, 178, doi:10.1186/s13287-024-03786-1.
48. Ward, C.L.; Sanchez Jr, C.J.; Pollot, B.E.; Romano, D.R.; Hardy, S.K.; Becerra, S.C.; Rathbone, C.R.; Wenke, J.C. Soluble Factors from Biofilms of Wound Pathogens Modulate Human Bone Marrow-Derived Stromal Cell Differentiation, Migration, Angiogenesis, and Cytokine Secretion. *BMC Microbiol.* **2015**, *15*, 75, doi:10.1186/s12866-015-0412-x.
49. Vyas, K.S.; Wong, L.K. Detection of Biofilm in Wounds as an Early Indicator for Risk for Tissue Infection and Wound Chronicity. *Ann. Plast. Surg.* **2016**, *76*, 127–131, doi:10.1097/SAP.0000000000000440.
50. Komori, T. Regulation of Osteoblast Differentiation by Runx2. In *Osteoimmunology*; Choi, Y., Ed.; Advances in Experimental Medicine and Biology; Springer US: Boston, MA, 2009; Vol. 658, pp. 43–49 ISBN 978-1-4419-1049-3.
51. Silvent, J.; Nassif, N.; Helary, C.; Azaïs, T.; Sire, J.-Y.; Guille, M.M.G. Collagen Osteoid-Like Model Allows Kinetic Gene Expression Studies of Non-Collagenous Proteins in Relation with Mineral Development to Understand Bone Biomineralization. *PLoS ONE* **2013**, *8*, e57344, doi:10.1371/journal.pone.0057344.
52. Xu, J.; Li, Z.; Hou, Y.; Fang, W. Potential Mechanisms Underlying the Runx2 Induced Osteogenesis of Bone Marrow Mesenchymal Stem Cells. Am. J. Transl. Res. 2015, 7, 2527–2535.
53. Liu, T.M.; Lee, E.H. Transcriptional Regulatory Cascades in Runx2-Dependent Bone Development. Tissue Eng. Part B Rev. 2013, 19, 254–263, doi:10.1089/ten.teb.2012.0527.
54. AlMoharib, H.S.; AlRowis, R.; AlMubarak, A.; Waleed Almadhoon, H.; Ashri, N. The Relationship between Matrix Metalloproteinases-8 and Peri-Implantitis: A Systematic Review and Meta-Analysis. Saudi Dent. J. 2023, 35, 283–293, doi:10.1016/j.sdentj.2023.03.012.

55. Sugawara, Y.; Suzuki, K.; Koshikawa, M.; Ando, M.; Iida, J. Necessity of Enzymatic Activity of Alkaline Phosphatase for Mineralization of Osteoblastic Cells. *Jpn. J. Pharmacol.* **2002**, *88*, 262–269, doi:10.1254/jjp.88.262.
56. Zohar, R.; Cheifetz, S.; McCulloch, C.A.G.; Sodek, J. Analysis of Intracellular Osteopontin as a Marker of Osteoblastic Cell Differentiation and Mesenchymal Cell Migration. *Eur. J. Oral Sci.* **1998**, *106*, 401–407, doi:10.1111/j.1600-0722.1998.tb02206.x.
57. Manolagas, S.C. Osteocalcin Promotes Bone Mineralization but Is Not a Hormone. *PLOS Genet.* **2020**, *16*, e1008714, doi:10.1371/journal.pgen.1008714.
58. Umeyama, R.; Yamawaki, T.; Liu, D.; Kanazawa, S.; Takato, T.; Hoshi, K.; Hikita, A. Optimization of Culture Duration of Bone Marrow Cells before Transplantation with a β-Tricalcium Phosphate/Recombinant Collagen Peptide Hybrid Scaffold. Regen. Ther. 2020, 14, 284–295, doi:10.1016/j.reth.2020.04.005.
59. Pullisaar, H.; Verket, A.; Szoke, K.; Tiainen, H.; Haugen, H.J.; Brinchmann, J.E.; Reseland, J.E.; Østrup, E. Alginate Hydrogel Enriched with Enamel Matrix Derivative to Target Osteogenic Cell Differentiation in TiO2 Scaffolds. J. Tissue Eng. 2015, 6, 2041731415575870, doi:10.1177/2041731415575870.
62. Han, Y.; Yang, J.; Fang, J.; Zhou, Y.; Candi, E.; Wang, J.; Hua, D.; Shao, C.; Shi, Y. The Secretion Profile of Mesenchymal Stem Cells and Potential Applications in Treating Human Diseases. Signal Transduct. Target. Ther. 2022, 7, 92, doi:10.1038/s41392-022-00932-0.
61. Cai, B.; Lin, D.; Li, Y.; Wang, L.; Xie, J.; Dai, T.; Liu, F.; Tang, M.; Tian, L.; Yuan, Y.; et al. N2-Polarized Neutrophils Guide Bone Mesenchymal Stem Cell Recruitment and Initiate Bone Regeneration: A Missing Piece of the Bone Regeneration Puzzle. Adv. Sci. 2021, 8, 2100584, doi:10.1002/advs.202100584.
62. Ebersole, J.L.; Peyyala, R.; Gonzalez, O.A. Biofilm-induced Profiles of Immune Response Gene Expression by Oral Epithelial Cells. *Mol. Oral Microbiol.* **2019**, *34*, omi.12251, doi:10.1111/omi.12251.
63. Yin, L.; Li, X.; Hou, J. Macrophages in Periodontitis: A Dynamic Shift between Tissue Destruction and Repair. *Jpn. Dent. Sci. Rev.* **2022**, *58*, 336–347, doi:10.1016/j.jdsr.2022.10.002.
64. Dieckow, S.; Szafrański, S.P.; Grischke, J.; Qu, T.; Doll-Nikutta, K.; Steglich, M.; Yang, I.; Häussler, S.; Stiesch, M. Structure and Composition of Early Biofilms Formed on Dental Implants Are Complex, Diverse, Subject-Specific and Dynamic. *Npj Biofilms Microbiomes* **2024**, *10*, 155, doi:10.1038/s41522-024-00624-3.
65. Khatri, M.; Bansal, M.; Puri, K.; Mehrotra, S.; Kumar, A.; Rehan, M. Evaluation of the Correlation between Interleukin 1β Levels in Peri-Implant Crevicular Fluid as an Adjunctive Diagnostic Marker with Clinical and Radiographic Parameters for Assessing the Peri-Implant Health Status. Natl. J. Maxillofac. Surg. 2022, 13, 421–429, doi:10.4103/njms.njms_337_21.
66. Severino, V.O.; Napimoga, M.H.; De Lima Pereira, S.A. Expression of IL-6, IL-10, IL-17 and IL-8 in the Peri-Implant Crevicular Fluid of Patients with Peri-Implantitis. Arch. Oral Biol. 2011, 56, 823–828, doi:10.1016/j.archoralbio.2011.01.006.
67. Lopes, G.; Sousa, C.; Silva, L.R.; Pinto, E.; Andrade, P.B.; Bernardo, J.; Mouga, T.; Valentão, P. Can Phlorotannins Purified Extracts Constitute a Novel Pharmacological Alternative for Microbial Infections with Associated Inflammatory Conditions? *PLoS ONE* **2012**, *7*, e31145, doi:10.1371/journal.pone.0031145.
68. Douglas, T.E.L.; Dokupil, A.; Reczyńska, K.; Brackman, G.; Krok-Borkowicz, M.; Keppler, J.K.; Božič, M.; Van Der Voort, P.; Pietryga, K.; Samal, S.K.; et al. Enrichment of Enzymatically Mineralized Gellan Gum Hydrogels with Phlorotannin-Rich *Ecklonia Cava* Extract Seanol® to Endow Antibacterial Properties and Promote Mineralization. *Biomed. Mater.* **2016**, *11*, 045015, doi:10.1088/1748-6041/11/4/045015.
69. Eom, S.-H.; Kim, Y.-M.; Kim, S.-K. Antimicrobial Effect of Phlorotannins from Marine Brown Algae. *Food Chem. Toxicol.* **2012**, *50*, 3251–3255, doi:10.1016/j.fct.2012.06.028.